

Research Paper

COVID-19 receptor and malignant cancers: Association of CTS_L expression with susceptibility to SARS-CoV-2

Lianmei Zhang^{1,2,3#}, Chunli Wei^{2#}, Dabing Li^{2,4#}, Jiayue He^{2#}, Shuguang Liu², Haoyue Deng², Jingliang Cheng², Jiaman Du², Xiaoyan Liu², Hanchun Chen⁵, Suan Sun³, Hong Yu^{1✉}, Junjiang Fu^{2✉}

1. Department of Pathology, Taizhou People's Hospital Affiliated to Nanjing University of Chinese Medicine, Taizhou, Jiangsu Province, China.
2. Key Laboratory of Epigenetics and Oncology, the Research Center for Preclinical Medicine, Southwest Medical University, Luzhou 646000, Sichuan Province, China.
3. Department of Pathology, The Affiliated Huai'an No. 1 People's Hospital of Nanjing Medical University, Huai'an 223300, Jiangsu Province, China.
4. Basic Medical School, Southwest Medical University, Luzhou 646000, Sichuan Province, China.
5. Department of Biochemistry, School of Life Sciences, Central South University, Changsha 410013, Hunan Province, China.

#These authors contributed equally to this work.

✉ Corresponding authors: Dr. Junjiang Fu, Key Laboratory of Epigenetics and Oncology, the Research Center for Preclinical Medicine, Southwest Medical University, Luzhou, Sichuan 646000, P R China. Tel/Fax: +86-830-3160283; E-mail: fujunjiang@swmu.edu.cn; Dr. Hong Yu; E-mail: yuhong13807@163.com.

© The author(s). This is an open access article distributed under the terms of the Creative Commons Attribution License (<https://creativecommons.org/licenses/by/4.0/>). See <http://ivyspring.com/terms> for full terms and conditions.

Received: 2021.12.17; Accepted: 2022.02.20; Published: 2022.03.06

Abstract

CTS_L is expressed by cancerous tissues and encodes a lysosomal cysteine proteinase that regulates cancer progression and SARS-CoV-2 entry. Therefore, it is critical to predict the susceptibility of cancer patients for SARS-CoV-2 and evaluate the correlation between disease outcomes and the expression of CTS_L in malignant cancer tissues. In the current study, we analyzed CTS_L expression, mutation rate, survival and COVID-19 disease outcomes in cancer and normal tissues, using online databases. We also performed immunohistochemistry (IHC) to test CTS_L expression and western blot to monitor its regulation by cordycepin (CD), and N6, N6-dimethyladenosine (m⁶2A), respectively. We found that CTS_L is conserved across different species, and highly expressed in both normal and cancer tissues from human, as compared to ACE2 or other proteinases/proteases. Additionally, the expression of CTS_L protein was the highest in the lung tissue. We show that the mRNA expression of CTS_L is 66.4-fold higher in normal lungs and 54.8-fold higher in cancer tissues, as compared to ACE2 mRNA expression in the respective tissues. Compared to other proteases/proteinases/convertases such as TMPRSS2 and FURIN, the expression of CTS_L was higher in both normal lungs and lung cancer samples. All these data indicate that CTS_L might play an important role in COVID-19 pathogenesis in normal and cancer tissues of the lungs. Additionally, the CTS_L-002 isoform containing both the inhibitor_I29 and Peptidase_C1 domains was highly prevalent in all cancers, suggesting its potential role in tumor progression and SARS-CoV-2 entry in multiple types of cancers. Further analysis of the expression of CTS_L mutant showed a correlation with FURIN and TMPRSS2, suggesting a potential role of CTS_L mutations in modulating SARS-CoV-2 entry in cancers. Moreover, high expression of CTS_L significantly correlated with a short overall survival (OS) in lung cancer and glioma. Thus, CTS_L might play a major role in the susceptibility of lung cancer and glioma patients to SARS-CoV-2 uptake and COVID-19 severity. Furthermore, CD or m⁶2A inhibited CTS_L expression in the cancer cell lines A549, MDA-MB-231, and/or PC3 in a dose dependent manner. In conclusion, we show that CTS_L is highly expressed in normal tissues and increased in most cancers, and CD or m⁶2A could inhibit its expression, suggesting the therapeutic potential of targeting CTS_L for cancer and COVID-19 treatment.

Key words: The CTS_L gene; Malignant cancers; SARS-CoV-2; COVID-19; Susceptibility; N6, N6-dimethyladenosine (m⁶2A); Cordycepin (CD)

Introduction

The CTS_L (*Cathepsin L*) gene, also known as *MEP*, *CATL*, and *CTSL1*, is located in the chromosome region 9q21.33. The GenBank access number for CTS_L gene is NM_001912.5 and CTS_L protein is NP_001903.1. The CTS_L gene encodes a 37,564 (Da)

lysosomal cysteine proteinase consisting of 333 amino acids, which plays a critical role in intracellular protein catabolism. CTS_L belongs to the peptidase C1 family, which forms a disulfide-linked dimer of heavy and light chains [1]. As a proteinase, the substrates of

CTSL include elastin, collagen, and alpha-1 protease inhibitor and thus it is implicated in several pathologic processes, including myofibril necrosis and tumor progression. Upregulation of CTS defense correlates with metastatic aggressiveness and poor prognosis in cancer patients [2]. CTS defense expression was shown to be elevated in glioblastoma multiforme (GBM) tissue as compared to the normal brain tissue [3]. Importantly, CTS defense can proteolytically cleave the S1 subunit on severe acute respiratory syndrome coronavirus 2 (SARS-CoV-2) spike protein, which is necessary for viral entry into the host cells [4-6]. Middle East Respiratory Syndrome (MERS) and Gingival overgrowth are some of the other diseases associated with CTS defense [7-9].

COVID-19 (coronavirus disease 2019) has quickly spread since December 2019 and the number of cases due to SARS-CoV-2 infection have been rising worldwide [10-13]. At the end of January 2022, more than 375 million people were diagnosed with SARS-CoV-2 infection and the confirmed deaths were over 5.6 million worldwide (<https://coronavirus.jhu.edu/>). The critical event promoting the entry of genetic material from SARS-CoV-2 into the host cells is the activation of S-protein by host proteinases/proteases, which enables its binding to the host cell receptors. The cleavage between the residues Thr696 and Met697 in S-protein domains of S1-S2 by CTS defense promotes the release of the viral genome into the host cells [14]. Previous *in vitro* studies have demonstrated that the inhibition of CTS defense decreases the entry of SARS-CoV-2 into the host cells by more than 76%, indicating the importance of CTS defense in mediating the viral entry. Therefore, targeting CTS defense could be a potential strategy for treating SARS-CoV-2 infection [15-17].

The nucleoside antimetabolite cordycepin (CD), derived from the fungal extracts of *Cordyceps militaris*, has been reported to show broad spectrum anti-viral, anti-cancer, anti-inflammatory, hepato-protective, antidepressant, and neuro-protective activity [18, 19]. CD showed strong binding affinities with SARS-CoV-2 S-protein and Mpro proteins [20]. CD was also reported to inhibit the expression of FURIN, a SARS-CoV-2 receptor, on cancer cell lines in a dose dependent manner [21]. N6,N6-Dimethyladenosine (m⁶A) is a modified ribonucleoside previously found in rRNA and also presented in tRNA from *mycobacterium bovis* Bacille Calmette-Guérin [22].

Regulation of CTS defense expression by Chinese medicine has shown its potential role in tumorigenesis, cancer progression and SARS-CoV-2 infection. However, the impact of CTS defense expression in SARS-CoV-2 infected cancer patients is still unknown. Thus, it is important to predict the susceptibility of

cancer patients for SARS-CoV-2 entry and the disease outcome by accessing the expression of CTS defense in different tumor tissues. It is also not known whether CD or m⁶A regulates CTS defense expression. In the current work, we analyzed the expression profile of CTS defense in different types of tumor tissues and matched normal tissues, in order to predict its potential role as a therapeutic marker. Moreover, *in vitro* studies showed that CD and m⁶A could suppress CTS defense expression.

Materials and Methods

Homology analysis

Homologs of CTS defense in humans (NP_001903.1 in protein and NM_001912.5 in gene in GenBank, Ensembl ID: Ensembl:ENSG00000135047) and others species were determined from the NCBI (National Center for Biotechnology Information) (https://www.ncbi.nlm.nih.gov/homologene?Db=homologene&C_md=Retrieve&list_uids=129366) as previously described [23, 24]. UniProtKB/Swiss was used to determine CTS defense domains (Prot: P07711).

Online databases for CTS defense expressions

The Human Protein Atlas (HPA) was used to predict the CTS defense gene and protein expressions in the normal and tumor tissues (<https://www.proteinatlas.org/ENSG00000135047-CTS defense>) [25-27]. The gene expression of CTS defense in multiple cancer tissues and matched normal tissues were performed from Genotype-Tissue Expression (GTEx) and The Cancer Genome Atlas (TCGA) databases using GEPIA 2 analysis (Gene Expression Profiling Interactive Analysis) (<http://gepia2.cancer-pku.cn/#analysis>) [28]. GEPIA 2 was also used to compare the gene expressions for FURIN, CTS defense and TMPRSS2 (*transmembrane protease serine 2*) in cancer tissues and matched normal tissues. For analysis of CTS defense isoform usage/distribution and structure of domains from different cancer tissues, GEPIA2 analysis was also conducted in the large datasets of TCGA and GTEx. Survival analysis of CTS defense expressions from TCGA database was also obtained from HPA.

CTS defense mutation analysis and effect on COVID-19 receptor expression

Gene mutation modules for CTS defense were performed by TIMER2.0 (<http://timer.compgenomics.org/>), and compared to the expression of other receptors, such as ADAM17 (ADAM Metallopeptidase Domain 17), HSPA5 (Heat Shock Protein Family A (Hsp70) Member 5), ACE2 (Angiotensin Converting Enzyme 2), TMPRSS2, FURIN, and CTS defense, in order to evaluate the importance of SARS-CoV-2 infection.

Immunohistochemistry (IHC) assays

The methods for immunohistochemistry (IHC) in formalin-fixed, paraffin-embedded lung and breast cancer tissue sections from Chinese patients were described previously [21, 26, 27, 29]. The CTSL antibody (Catalog No. ABIN1172740) for IHC was purchased from antibodies-online GmbH (Aachen, Germany). The color images of the antibody stained tissue sections were obtained using microscopy. The immune positive rate was generally based on the percentage of positive cells and the staining intensity. It was divided into 0, < 5%; 1, 5% ~ 25%; 2, 25% ~ 50%; 3, 50% ~ 75% and 4, > 75%. Immunohistochemical color intensity was divided into: 1, weak; 2, medium; and 3, intense. The two scores were multiplied, and the product was defined as the immunohistochemical score. This evaluation was carried out by two independent pathologists in a blinded fashion.

Western blotting and semi-quantitative RT-PCR analysis

Cordycepin (CD) was purchased from Must Bio-Technology Co. Ltd in Chengdu, Sichuan, P. R. China. The lung cancer cell line A549, prostate cancer cell line PC3 and triple-negative breast cancer cell line MDA-MB-231 were used in this study. Western blotting for CTSL protein expression was conducted in A549, MDA-MB-231 and PC3 with CD treatments (0, 10 μ m, 20 μ m, 40 μ m) for 24 hours, which were described previously [21]. PC3 prostate cancer cells were treated with N6, N6-dimethyladenosine (m⁶₂A) (0, 10 μ m, 20 μ m, 40 μ m) for 24 hours. The CTSL antibody for western blotting was purchased from Abcam (Catalog No. ab200738). Tubulin (anti- β -

Tubulin) antibody (Sigma-Aldrich, catalog No. T0198) was used as the internal control. Western blotting was described previously [29-31]. The semi-quantitative RT-PCR analysis was also performed using the above treated cells. Primers for RT-PCR were as follows: RT-CTSL-L, 5'-agggaaaggaaacacagctt-3', RT-CTSL-R, 5'-aagcccaacaagaaccacac-3'. The amplified size was 223bp. GAPDH was used as an internal control. All experiments were repeated three times.

Cycloheximide (CHX) chase assays

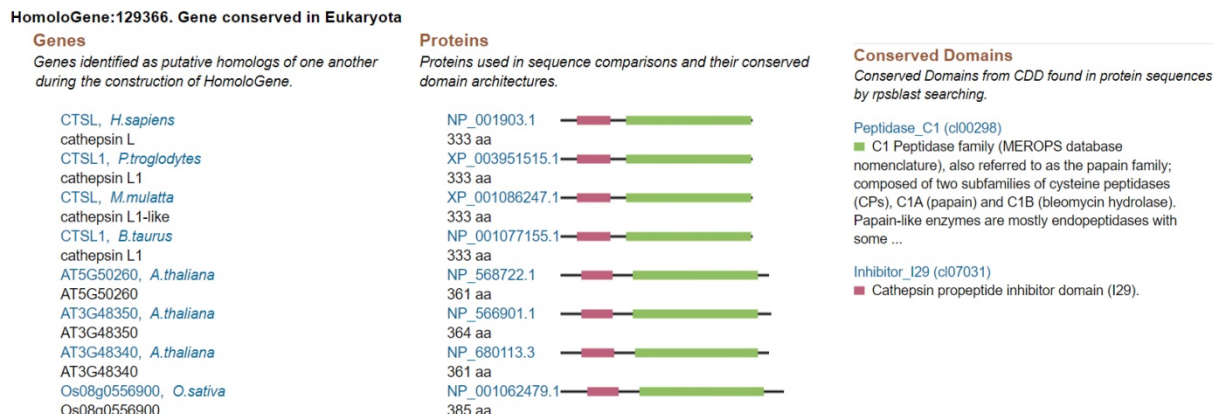
MDA-MB-231 cell line was used for cycloheximide (CHX, Catalog No. A49960, ACMEC in Shanghai, China) treatment, for the indicated time with or without CD treatment (CD treated for 1 hour at first). Following this, western blotting for CTSL was performed as described above. Tubulin antibody was also used as an internal control. The intensities for CTSL and tubulin bands were quantified by densitometry and analyzed using adobe photoshop CS3 software [32]. The experiments were repeated three times.

Results

Conservation of CTSL across species

Homology analysis revealed the conservation of CTSL protein across different species such as chimpanzee, Rhesus monkey, cow, *A. thaliana*, and rice, suggesting a potential role of CTSL in SARS-CoV-2 entry in multiple species (Figure 1A). Structural analysis of CTSL showed two conserved domains, including Inhibitor_I29 (Cathepsin propeptide inhibitor domain (I29)) and Peptidase_C1 (Papain family cysteine protease) (Figure 1B).

A



B



Figure 1. Homologs and conservation of the CTSL protein. A. CTSL expression from different species. **B.** Conserved domains of CTSL.

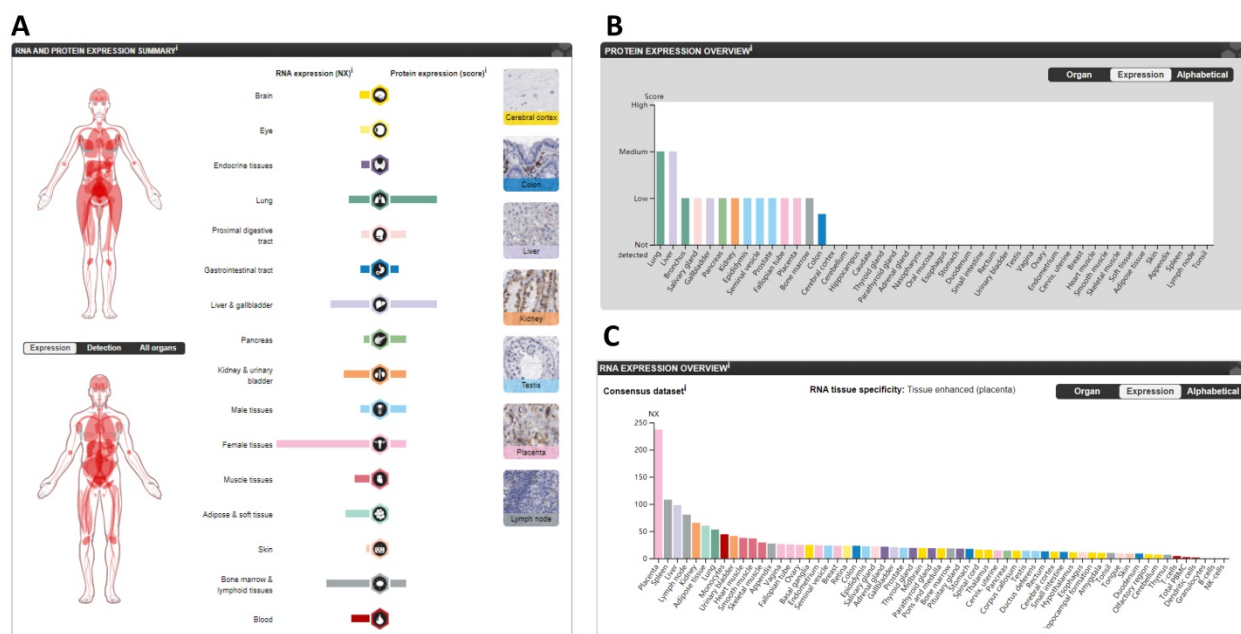


Figure 2. The expression of CTS_L in normal tissues in humans. **A.** The summary of CTS_L expression in organs. **B.** The CTS_L protein expression in normal tissues. **C.** The CTS_L mRNA expression in normal tissues. NX, consensus normalized expression.

CTSL expression varies across different “normal” tissues

The protein and mRNA expression profiles of CTS defense in different tissues from the HPA are summarized in Figure 2A. CTS defense protein levels, based on a high, medium, low, or not detected score, revealed two tissues (lungs and livers) with medium expression; eleven tissues with low expression; one tissue (colon) with lower expression; and thirty-one tissues showed no detectable expression (Figure 2B). For mRNA levels, the consensus dataset consisted of normalized expression (NX) levels in different tissue types by combining the transcriptomic datasets of the HPA and GTEx using the internal normalization pipeline. CTS defense mRNA levels from these consensus datasets revealed a high expression in the placenta with 237.0 NX, followed by the spleen (108.1 NX), and the liver (98.0 NX); noticeably, the lungs had the seventh highest expression (53.1 NX). B-cells and NK-cells were found to have the lowest CTS defense mRNA expression (Figure 2C). Therefore, our findings show that the expression levels of CTS defense varies across different human tissues. High expression of CTS defense in the lungs indicates its importance for viral entry into the lungs.

CTSL isoform usage and structure in cancer tissues

Expression of different ACE2 isoforms in the airway epithelium contributes differentially to viral susceptibility [33]; isoforms for other SARS-CoV-2 receptors may also play similar roles. GEPIA2

database in 33 types of tumor tissues showed three isoforms (Figure 3A). The isoforms CTSI-001 and CTSI-002 contain both the inhibitor_I29 and Peptidase_C1 domains, which is same as shown in Figure 1B. But isoform CTSI-004 only contains the inhibitor_I29 and half of the Peptidase_C1 domain. Information for the other three isoforms ENST-00000375894.9 (CTSI-005), ENST00000482054.1 (CTSI-006), and ENST00000495822.1 (CTSI-003) were missing. As for CTSI isoform prevalence, we noticed that all six isoforms were expressed, but at different levels, with CTSI-006 and CTSI-001 being the highest, followed by CTSI-002; and CTSI-006 was the lowest in different tumors (Figure 3B). The usage of isoform CTSI-002 was very high in all cancers; the other five isoforms were found to be minimally expressed (Figure 3C). Based on the distribution of CTSI isoform expression and usage, we concluded that CTSI-002 might play a major role in tumor progression and SARS-CoV-2 entry in different kinds of tumor tissues.

CTSL mutation analysis in different tumors showed the highest mutation rate in UCEC (Uterine Corpus Endometrial Carcinoma) ($20/531=3.77\%$), followed by DLBC (Lymphoid Neoplasm Diffuse Large B-cell Lymphoma) ($1/37=2.70\%$), and HNSC (Head and Neck squamous cell carcinoma) showed the lowest ($1/509=0.19\%$) mutation rate (Figure 3D). Further analysis of the correlation of mutant *CTSL* expression with other proteases/proteinases or convertases such as *FURIN* and *TMPRSS2* were performed. This analysis is mainly based on the log₂ fold expression changes of interesting genes in each

cancer type. We report that the mutant CTS_L expression correlates with elevated FURIN expression in multiple cancers, while there is no such correlation in a few cancers (Figure 3E, FURIN panel); but TMPRSS2 showed either increase or decrease in a few cancers (Figure 3E, TMPRSS2 panel). Considering TMPRSS2 is mainly expressed in prostate cancer, we conclude that CTS_L mutations primarily correlated with FURIN expression, which might further regulate SARS-CoV-2 entry in cancers.

The subcellular localization of CTS_L in cells

To determine the subcellular spatial distribution of CTS_L in human cells, immunofluorescence (IF) staining was analyzed. The IF staining showed CTS_L localization at the Golgi apparatus and vesicles of sparkle signals (Supplementary Figure 1). This subcellular localization at Golgi apparatus and vesicles implies the possible role of CTS_L in the cleavage of S-protein, enabling its binding to the host receptors.

CTS_L expression in lung cancer and breast cancer

We also performed IHC in the lung and breast tumors and matched normal tissues. The representative results are shown in Figure 4. We report that IHC staining in the cytoplasm shows moderate intensity in both the normal lung (Figure 4A) and breast tissues (Figure 4D), whereas, slight increase in lung cancer tissues (Figure 4B) and

significant increase in breast cancer tissues (Figure 4E) were observed. However, in the absence of antibody, there was no staining detected in the lung and breast cancer tissues (Figure 4C & F).

Pan-cancer expression of CTS_L in malignant cancer tissues and matched normal samples

Going forward, we quantitatively compared CTS_L mRNA expression profiles from thirty-three types of cancers and their matched normal tissues, including those of breast and lung. The results revealed that, all types of cancer tissues showed CTS_L expression; the highest levels were found in SKCM (Skin Cutaneous Melanoma) (Figure 5A). Although most tumor tissues showed an elevated expression of CTS_L mRNA (Figure 5A), it was significantly elevated in eight tumor types, including DLBC, ESCA (Esophageal carcinoma), LGG (Brain Lower Grade Glioma), GBM (Glioblastoma multiforme), PAAD (Pancreatic adenocarcinoma), SKCM, STAD (Stomach adenocarcinoma) and THYM (Thymoma) (Figure 5A in red, 5B, p<0.01). On the other hand, CTS_L mRNA levels were dramatically decreased in three other cancer types, including COAD (Colon adenocarcinoma), LAML (Acute myeloid leukemia) and READ (Rectum adenocarcinoma) (Figure 5A in green, 5C, p<0.01). In conclusion, our findings suggest that CTS_L may play an important role in the uptake of SARS-CoV-2 in most of the tumor tissues.

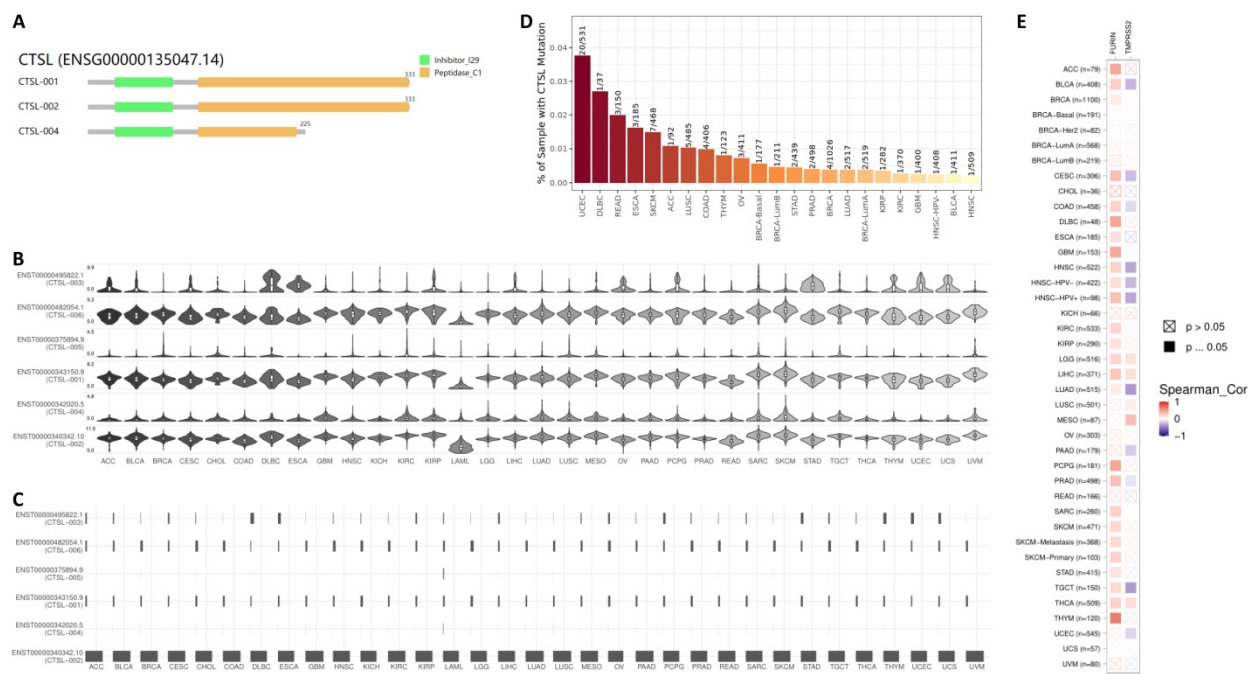


Figure 3. The usage and the structure of CTS_L isoforms in different types of cancers. **A.** Structure of CTS_L isoforms is shown. Three isoforms and two visualized domains are shown in an interactive plot. Note: information for the following 3 isoforms are missing: ENST00000375894.9, ENST00000482054.1 and ENST00000495822.1. **B & C.** Usage of different CTS_L isoforms. The profiles for the distribution of CTS_L expression are shown with violin plot in panel B, and isoform usage is shown with bar plot in panel C. The X axis presents isoforms, whereas the Y axis presents the respective cancer types. **D.** Mutation status for CTS_L in different tumors from TCGA. **E.** The heat maps show the log2 fold expression changes of FURIN and TMPRSS2 in each tumor type. The full names of cancers are shown in right panel of Figure 6.

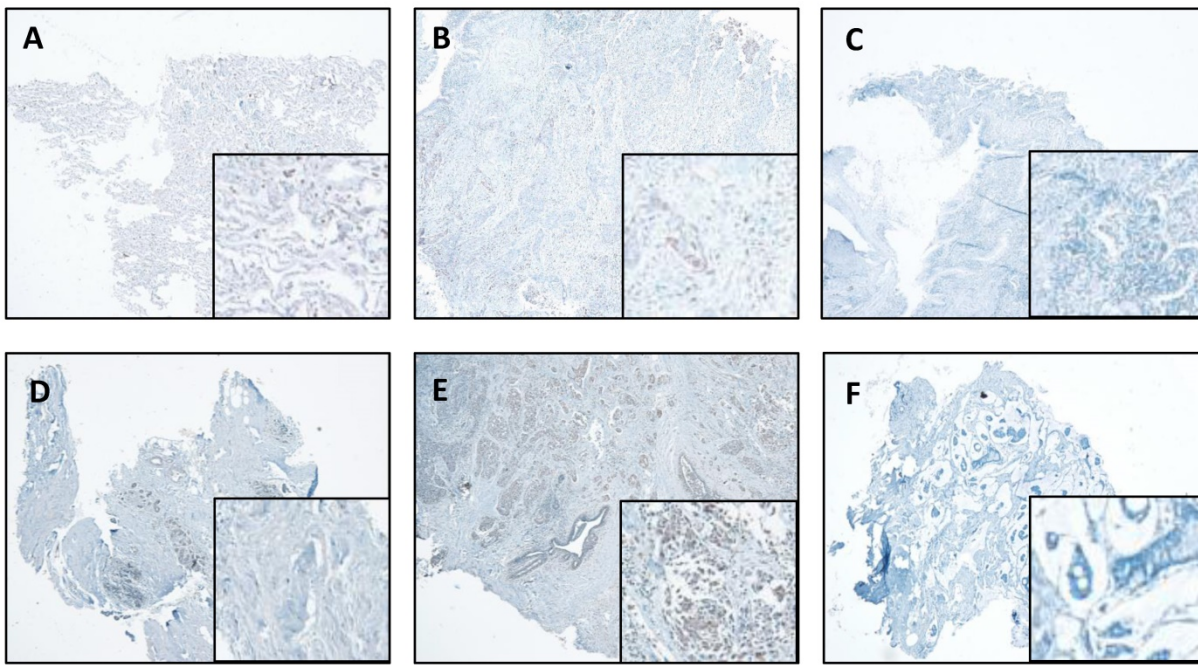


Figure 4. CTSL expression in normal and tumor tissues of the lung and breast. **A.** Representative staining for normal lung tissue from a lung cancer patient. **B.** Representative staining for cancer tissue from a lung cancer patient. **C.** No antibody control sample for normal lung tissue. **D.** Representative staining for normal breast tissues in a breast cancer patient. **E.** Representative staining for cancer tissue from a breast cancer patient. **F.** No antibody control sample for breast cancer tissue. 40X. Enlarged images are presented in the right corners of A-F, respectively. Note that the expression levels are based on the intensity of the staining and the percentage of positive cells.

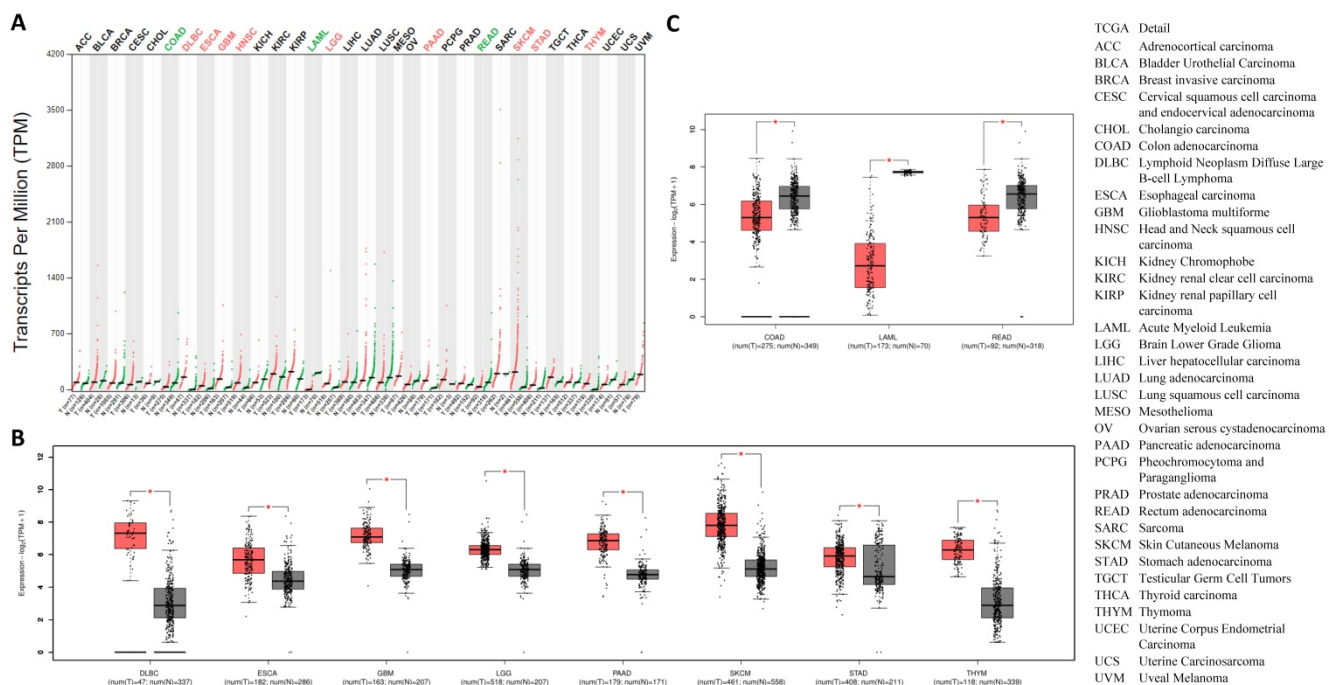


Figure 5. The expression of CTSL in tumor tissues and the corresponding normal tissues. **A.** CTSL expressions in 33 types of cancer tissues (red files) and the corresponding normal tissues (green files). Green in names indicates decreased expression whereas red in names indicates decreased expression in cancer tissues compared to the corresponding normal tissues. **B.** Expression profiles for CTSL in eight tumor tissues and their corresponding normal tissues. **C.** Expression profiles for CTSL in three tumor tissues and their corresponding normal tissues (*: $p < 0.01$). The cancer tissue is in red, the normal tissue is in grey. Tissue-wise expressions are used as box plots. Right panel shows the cancerous full names.

Comparison of the expression levels of ADAM17, HSPA5, ACE2, TMPRSS2, FURIN and CTSL in tumor and normal tissues

ADAM17, HSPA5, ACE2, TMPRSS2, and FURIN

are all viral receptors, which are essential for SARS-CoV-2 uptake [23, 28, 34]. The expression levels of these genes were analyzed in different tumor tissues from TCGA datasets. We found that mRNA expression of HSPA5 was the highest, followed by

FURIN and *CTSL* in the majority of the tumor tissues, and *ACE2* expression was the lowest (Figure 6A), demonstrating that *CTSL* might facilitate tumorigenesis and SARS-CoV-2 entry in most cancers.

ACE2 was reported as the most critical functional receptor for SARS-CoV-2 entry into the lungs [35, 36]. Thus, we compared the expression of *CTSL* and *ACE2* mRNA in normal lungs and lung cancers. The results showed that *ACE2* expression was approximately 0.8 NX and 0.9 FPKM in normal lungs and lung cancers, respectively. However, *CTSL* expression value was 53.1 NX and 49.3 FPKM, in the respective tissues, which was 66.4-fold ($53.1/0.8=66.4$) higher than *ACE2* mRNA expression in normal lungs (Figure 6B), and 54.8-fold ($49.3/0.9=54.8$) higher than *ACE2* mRNA expression in the lung cancers (Figure 6C). *CTSL*, *TMPRSS2* and *FURIN* belong to proteinase/protease family. We further compared the expression levels of *CTSL*, *TMPRSS2*, and *FURIN* in normal lungs and lung cancers. We found the

expression of *CTSL* to be the highest in both tissues (Figure 6C & D). In conclusion, these data demonstrate that *CTSL* may play an important role in COVID-19 pathogenesis in normal and cancerous lung tissues.

Prognostic value of *CTSL* expression for overall survival in cancer patients

We analyzed the clinical correlation between *CTSL* expression and overall survival (OS) outcomes in HPA (Figure 7). We found that a high expression of *CTSL* was significantly correlated with a short OS in lung cancer (Figure 7A, $p<0.001$) and glioma patients (Figure 7B, $p<0.001$). On the other hand, high *CTSL* expression significantly correlated with a long OS in renal cancer patients (Figure 7C, $p<0.001$). Thus, *CTSL* expression may be an unfavorable prognostic marker for survival in lung cancer and glioma patients, and a favorable prognostic marker for survival in renal cancer patients.

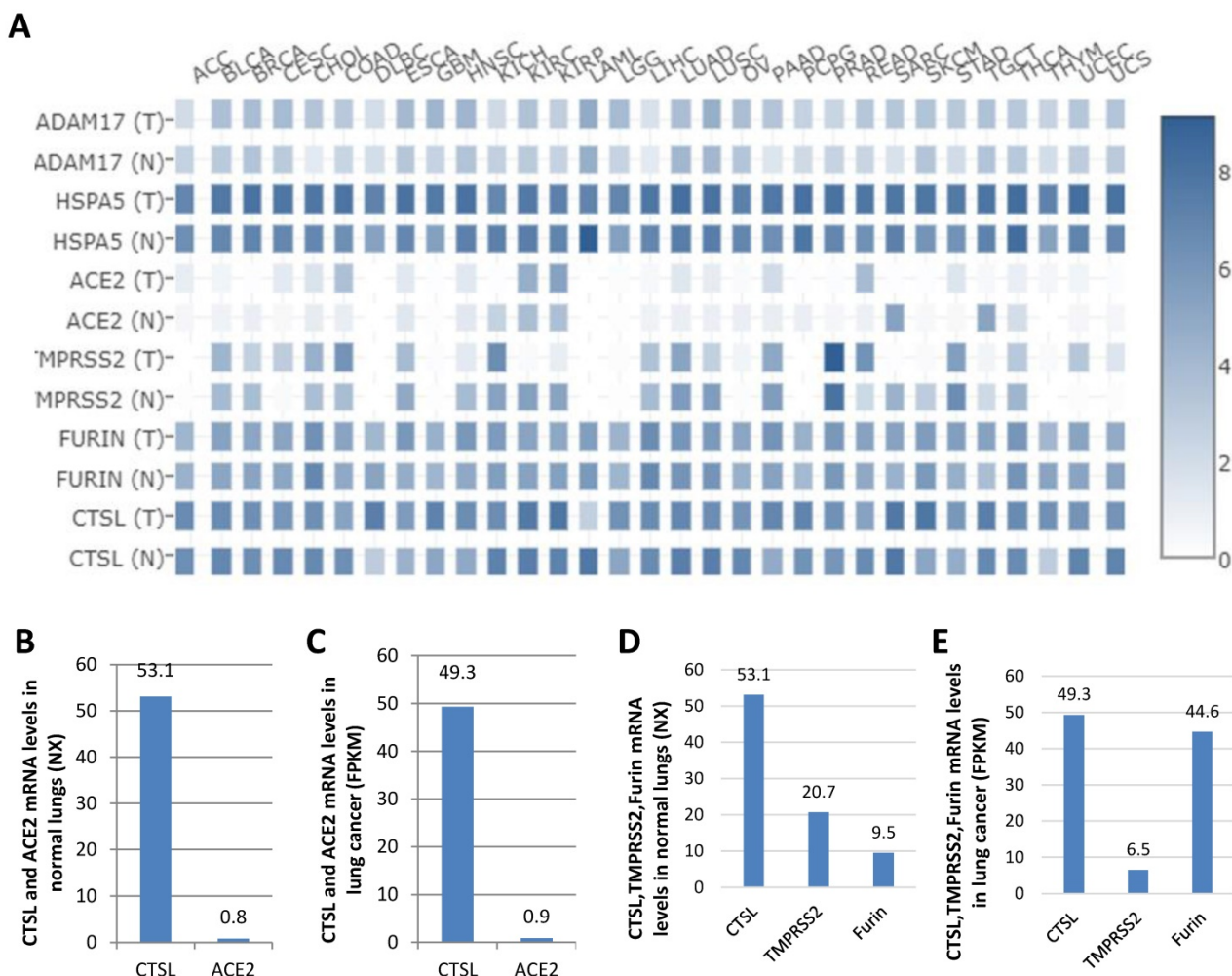


Figure 6. Comparison of the mRNA expression levels of ADAM17, HSPA5, ACE2, TMPRSS2, FURIN and CTS in thirty-one cancers and their matched normal tissues. **A.** Comparison of mRNA expression of ADAM17, HSPA5, ACE2, TMPRSS2, FURIN and CTS in 31 tumors and their matched normal tissues. “T” represents cancer tissues and “N” represents normal tissues. **B.** Comparison of mRNA expression of between ACE2 and CTS in normal tissues of the lungs. **C.** Comparison of mRNA expression between ACE2 and CTS in cancer tissues of the lungs. **D.** Comparison of mRNA expression between TMPRSS2, FURIN and CTS in normal tissues of the lungs. **E.** Comparison of mRNA expression between TMPRSS2, FURIN and CTS in cancer tissues of the lungs. The consensus dataset consists of normalized expression (NX) levels from different tissue types by combining the transcriptomic datasets of HPA and GTEx, using the internal normalization pipeline, or relative expression levels.

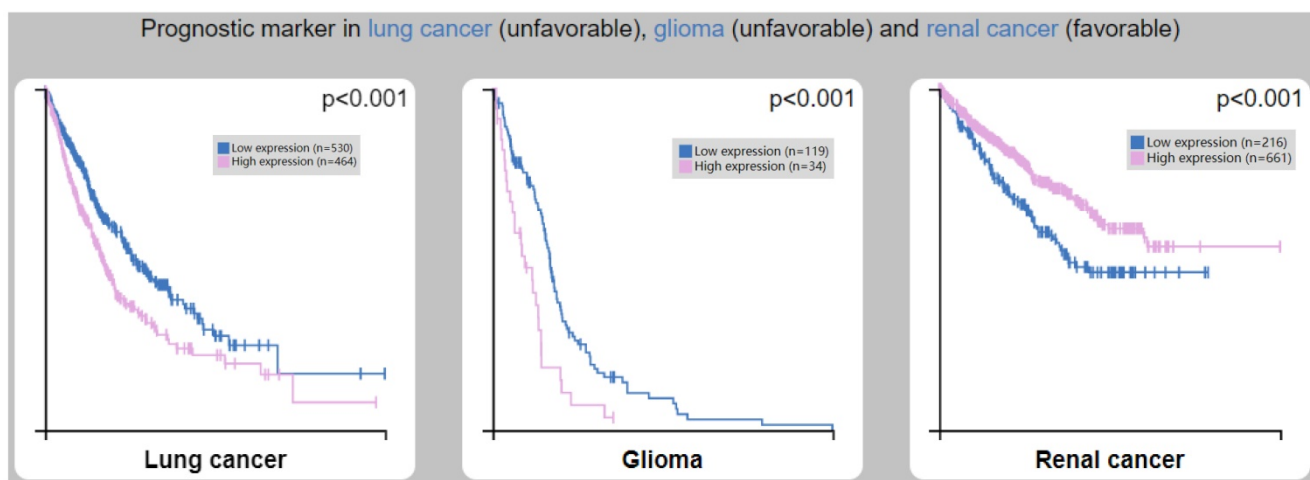


Figure 7. Correlation between CTSI expression and overall survival (OS) in patients with lung cancer (left panel), glioma (middle panel) and renal cancer (right panel). Note: Based on the FPKM (Fragments Per Kilobase Million) value of the CTSI gene, cancer patients were classified into two groups (high and low expression) and the correlations between expression level and patient survival were evaluated.

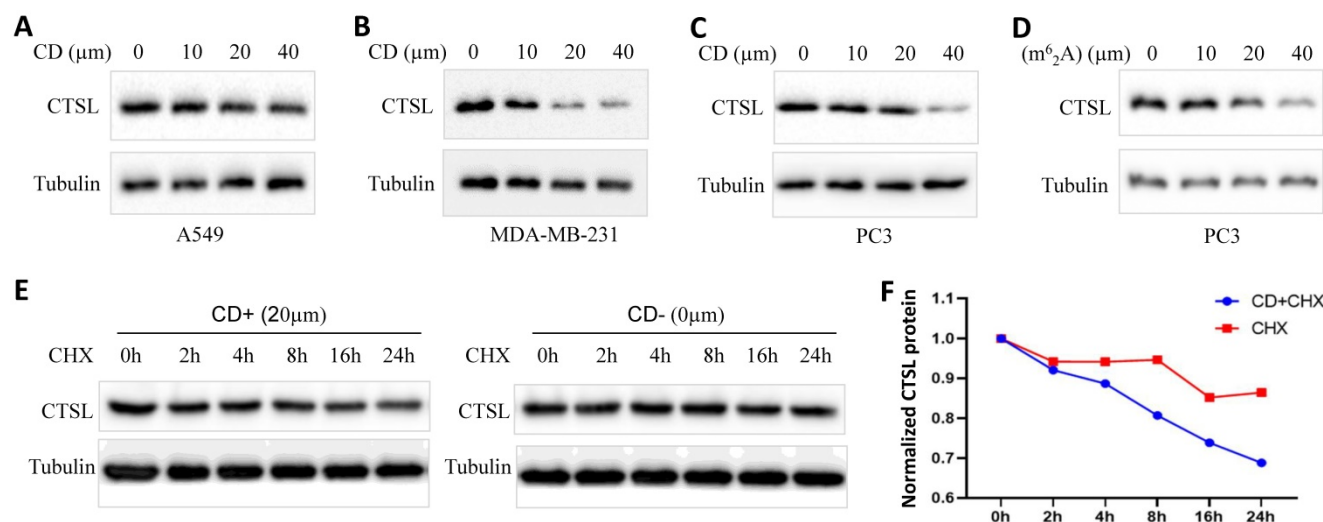


Figure 8. CD or m⁶A suppresses CTSI expression in cancer cell lines. **A.** CTSI protein levels after CD treatment in A549 lung cancer cell line. **B.** CTSI protein levels after CD treatment in MDA-MB-231 triple-negative breast cancer cell line. **C.** CTSI protein levels after CD treatment in PC3 prostate cancer cell line. **D.** CTSI protein levels after N6, N6-dimethyladenosine (m⁶A) treatment in prostate cancer cell line PC3. **E.** CTSI protein stability after CHX treatment with or without CD treatment. Left panel shows CD treatment, right panel shows without CD treatment. **F.** The quantitative results from E. Red line shows CHX treatment only, blue line shows CHX treatment together with CD treatment. The final concentration for CHX treatments were 40 μ g/ml.

Regulation of CTSI protein expression by Cordycepin (CD) or N6, N6-dimethyl-adenosine (m⁶A) in cancer cell lines

To explore the possibility of using CD or m⁶A as therapeutics against SARS-CoV-2, we analyzed the change in the expression of CTSI protein in cancer cell lines treated with these agents (Figure 8). We found that CD inhibited CTSI protein levels in a dose dependent manner in the lung cancer cell line A549, triple-negative breast cancer cell line MDA-MB-231, and prostate cancer cell line PC3, respectively (Figure 8A-C). However, treatment with CD did not cause any change in CTSI mRNA levels in the same cell lines (Supplementary Figure 2 and data not shown). m⁶A inhibited CTSI protein levels in a dose

dependent manner in the prostate cancer cell line PC3 (Figure 8D). These data indicate that CD inhibits CTSI protein levels at the translational level, potentially by degrading CTSI protein. Following this, we performed chase assays with CHX treatment, with and without CD treatments, in MDA-MB-231 cell line. The results showed that, CD treatment reduced the stability of CTSI protein (Figure 8E & F), suggesting that CD degraded CTSI protein. In conclusion, these results suggest that both CD and m⁶A might have a therapeutic potential as anti-SARS-CoV-2 agents through the suppression of CTSI protein expression.

Discussion

Cancer patients are more susceptible to

SARS-CoV-2 infection than those without cancer, and consequently are more likely to become severely ill or die when suffering from this viral infection [37–40]. Previous systematic reviews have reported an increased fatality in COVID-19 patients with cancer than those without cancer [39, 41]. Given this discrepancy, we sought to evaluate the expression levels of viral entry receptors in various cancer tissues, as cancerous pathology might affect COVID-19 susceptibility and illness [42, 43].

In this study, we found *CTSL* to be highly conserved across different species. We also found it to be highly expressed in normal and cancer tissues, especially in comparison to ACE2, an important receptor for SARS-CoV-2, as well as in comparison to other proteases. *CTSL* expression was found to be the highest in the lungs. We further compared the expression of *CTSL* and ACE2 mRNA in normal lungs and lung cancers and found that *CTSL* expression was 66.4-fold higher in normal lungs and 54.8-fold higher in lung cancer tissues, as compared to ACE2 mRNA levels in the respective tissues. By further comparison of *CTSL*, TMPRSS2, and FURIN, all of which are proteinase/protease/convertases [43, 44], we found the expression of *CTSL* to be the highest in both in normal lungs and lung cancers. All these data indicate a potential role of *CTSL* in COVID-19 pathogenesis in normal and cancerous tissues of the lungs. Furthermore, the *CTSL*-002 isoform containing both inhibitor_I29 and Peptidase_C1 domains is highly expressed in all cancers, suggesting its potential role in tumor progression and SARS-CoV-2 entry. We further analyzed the correlation between *CTSL* mutations and the expression of other proteases/proteinases/convertases such as FURIN and TMPRSS2, and found a positive correlation between *CTSL* and FURIN expression in multiple cancers. Thus *CTSL* mutations may further regulate SARS-CoV-2 entry in cancer tissue. Of note, we did not find any promoter methylation modification in the pan-cancer analysis. In the clinical setting, we found that high expression of *CTSL* was significantly correlated with a short OS in lung cancer and glioma patients. Thus *CTSL* may play a vital role in the susceptibility to SARS-CoV-2 entry and severity of COVID-19 clinical symptoms, particularly in lung cancer and in glioma patients.

CTSL is known to play a role in cancer invasion and metastasis, inflammation, renal disease, diabetes, bone diseases, atherosclerosis, viral infection, as well as other diseases. *CTSL* inhibitors or chloroquine has been shown to significantly reduce the viral replication. Therefore, *CTSL* could be a therapeutic target for both cancers and COVID-19 [15, 45]. *In vitro* expression analysis showed that CD or m⁶A

suppressed *CTSL* protein expression in a dose dependent manner. This is the first study identifying the inhibition of *CTSL* by nucleoside derivatives, CD and m⁶A, suggesting their role as anti-SARS-CoV-2 agents through *CTSL* inhibition.

Conclusions

CTSL expression was high in normal tissues and was increased in multiple cancer types. Both CD and m⁶A suppressed its expression, implying their therapeutic potential in preventing SARS-CoV-2 invasion and cancer progression. Our study highlights the value of targeting *CTSL* as a therapeutic strategy to combat cancer and COVID-19 pandemic.

Supplementary Material

Supplementary figures.

<https://www.ijbs.com/v18p2362s1.pdf>

Acknowledgments

This work was supported by the Scientific Research Project Foundation of Health Department, Jiangsu of China (grant no. H2017075), the Innovation Team Project Foundation of Taizhou People's Hospital (grant no. CXTDB201904), the Talent Startup Foundation of Southwest Medical University (grant no. 00040150), the Postdoctoral Startup Foundation of Southwest Medical University (grant no. 00040182), the Research Foundation of Luzhou City (grant no. 2021-SYF-37), the Foundation of Southwest Medical University (grant nos. 2021ZKMS004, 41/00160217), and in part by the National Natural Science Foundation of China (grant nos. 81672887 and 82073263).

Ethics approval

The study was approved by the Ethical Committee of Southwest Medical University and Huai'an People's Hospital Affiliated to Nanjing Medical University. Informed consent was obtained from patients.

Author Contributions

L. Z., D. L., J. H., H. D., J.D., S. L. did IHC, cell culture, western blotting, RT-PCR, collected and analyzed the data. J. F., S. S. and H. Y. designed and supervised the project. J.F. wrote and edited the manuscript. J. F., H.Y. and L.Z. revised the manuscript.

Competing Interests

The authors have declared that no competing interest exists.

References

- Fujishima A, Imai Y, Nomura T, Fujisawa Y, Yamamoto Y, Sugawara T. The crystal structure of human cathepsin L complexed with E-64. *FEBS Lett.* 1997; 407: 47-50.
- Sudhan DR, Siemann DW. Cathepsin L targeting in cancer treatment. *Pharmacol Ther.* 2015; 155: 105-16.
- Dong Q, Li Q, Duan L, Wang H, Yan Y, Yin H, et al. Expressions and significances of CTSL, the target of COVID-19 on GBM. *J Cancer Res Clin Oncol.* 2021. doi: 10.1007/s00432-021-03843-9.
- Huang IC, Bosch BJ, Li F, Li W, Lee KH, Ghiran S, et al. SARS coronavirus, but not human coronavirus NL63, utilizes cathepsin L to infect ACE2-expressing cells. *J Biol Chem.* 2006; 281: 3198-203.
- Bosch BJ, Bartelink W, Rottier PJ. Cathepsin L functionally cleaves the severe acute respiratory syndrome coronavirus class I fusion protein upstream of rather than adjacent to the fusion peptide. *J Virol.* 2008; 82: 8887-90.
- Zhao MM, Yang WL, Yang FY, Zhang L, Huang WJ, Hou W, et al. Cathepsin L plays a key role in SARS-CoV-2 infection in humans and humanized mice and is a promising target for new drug development. *Signal Transduct Target Ther.* 2021; 6: 134.
- Simmons G, Gosalia DN, Rennekamp AJ, Reeves JD, Diamond SL, Bates P. Inhibitors of cathepsin L prevent severe acute respiratory syndrome coronavirus entry. *Proc Natl Acad Sci U S A.* 2005; 102: 11876-81.
- Matsuyama S, Shirato K, Kawase M, Terada Y, Kawachi K, Fukushi S, et al. Middle East Respiratory Syndrome Coronavirus Spike Protein Is Not Activated Directly by Cellular Furin during Viral Entry into Target Cells. *J Virol.* 2018; 92.
- Nishimura F, Naruishi H, Naruishi K, Yamada T, Sasaki J, Peters C, et al. Cathepsin-L, a key molecule in the pathogenesis of drug-induced and I-cell disease-mediated gingival overgrowth: a study with cathepsin-L-deficient mice. *Am J Pathol.* 2002; 161: 2047-52.
- Wang C, Horby PW, Hayden FG, Gao GF. A novel coronavirus outbreak of global health concern. *Lancet.* 2020; 395: 470-3.
- Zheng J. SARS-CoV-2: an Emerging Coronavirus that Causes a Global Threat. *International journal of biological sciences.* 2020; 16: 1678-85.
- Deng CX. The global battle against SARS-CoV-2 and COVID-19. *International journal of biological sciences.* 2020; 16: 1676-7.
- Coutard B, Valle C, de Lamballerie X, Canard B, Seidah NG, Decroly E. The spike glycoprotein of the new coronavirus 2019-nCoV contains a furin-like cleavage site absent in CoV of the same clade. *Antiviral Res.* 2020; 176: 104742.
- Smieszek SP, Przychodzen BP, Polymeropoulos MH. Amantadine disrupts lysosomal gene expression: A hypothesis for COVID19 treatment. *Int J Antimicrob Agents.* 2020; 55: 106004.
- Gomes CP, Fernandes DE, Casimiro F, da Mata GF, Passos MT, Varela P, et al. Cathepsin L in COVID-19: From Pharmacological Evidences to Genetics. *Front Cell Infect Microbiol.* 2020; 10: 589505.
- Prasad K, Ahamed S, Gupta D, Kumar V. Targeting cathepsins: A potential link between COVID-19 and associated neurological manifestations. *Helix.* 2021; 7: e08089.
- Muralidhar S, Gopal G, Visaga Ambi S. Targeting the viral-entry facilitators of SARS-CoV-2 as a therapeutic strategy in COVID-19. *J Med Virol.* 2021; 93: 5260-76.
- Wei C, Yao X, Jiang Z, Wang Y, Zhang D, Chen X, et al. Cordycepin Inhibits Drug-resistance Non-small Cell Lung Cancer Progression by Activating AMPK Signaling Pathway. *Pharmacological research.* 2019; 144: 79-89.
- Panya A, Songprakhon P, Panwong S, Jantakee K, Kaewkod T, Tragoopua Y, et al. Cordycepin Inhibits Virus Replication in Dengue Virus-Infected Vero Cells. *Molecules.* 2021; 26.
- Verma AK, Aggarwal R. Repurposing potential of FDA-approved and investigational drugs for COVID-19 targeting SARS-CoV-2 spike and main protease and validation by machine learning algorithm. *Chem Biol Drug Des.* 2021; 97: 836-53.
- Li D, Liu X, Zhang L, He J, Chen X, Liu S, et al. COVID-19 disease and malignant cancers: The impact for the furin gene expression in susceptibility to SARS-CoV-2. *International journal of biological sciences.* 2021; 17: 3954-67.
- Chan CT, Chionh YH, Ho CH, Lim KS, Babu IR, Ang E, et al. Identification of N6,N6-dimethyladenosine in transfer RNA from *Mycobacterium bovis* Bacille Calmette-Guerin. *Molecules.* 2011; 16: 5168-81.
- Fu J, Zhou B, Zhang L, Balaji KS, Wei C, Liu X, et al. Expressions and significances of the angiotensin-converting enzyme 2 gene, the receptor of SARS-CoV-2 for COVID-19. *Molecular biology reports.* 2020; 47: 4383-92.
- Fu J, Wei C, He J, Zhang L, Zhou J, Balaji KS, et al. Evaluation and characterization of HSPA5 (GRP78) expression profiles in normal individuals and cancer patients with COVID-19. *International journal of biological sciences.* 2021; 17: 897-910.
- Uhlen M, Zhang C, Lee S, Sjostedt E, Fagerberg L, Bidkhorri G, et al. A pathology atlas of the human cancer transcriptome. *Science.* 2017; 357.
- Thul PJ, Akesson L, Wiking M, Mahdessian D, Geladaki A, Ait Blal H, et al. A subcellular map of the human proteome. *Science.* 2017; 356.
- Uhlen M, Fagerberg L, Hallstrom BM, Lindskog C, Oksvold P, Mardinoglu A, et al. Proteomics. Tissue-based map of the human proteome. *Science.* 2015; 347: 1260419.
- Tang Z, Li C, Kang B, Gao G, Li C, Zhang Z. GEPIA: a web server for cancer and normal gene expression profiling and interactive analyses. *Nucleic acids research.* 2017; 45: W98-W102.
- Zhang L, Yang M, Gan L, He T, Xiao X, Stewart MD, et al. DLX4 upregulates TWIST and enhances tumor migration, invasion and metastasis. *Int J Biol Sci.* 2012; 8: 1178-87.
- Zhou J, Imani S, Shasaltaneh MD, Liu S, Lu T, Fu J. PIK3CA hotspot mutations p. H1047R and p. H1047L sensitize breast cancer cells to thymoquinone treatment by regulating the PI3K/Akt1 pathway. *Mol Biol Rep.* 2021.
- Fu J, Qin L, He T, Qin J, Hong J, Wong J, et al. The TWIST1/Mi2/NuRD protein complex and its essential role in cancer metastasis. *Cell Res.* 2011; 21: 275-89.
- Wei C, Cheng J, Zhou B, Zhu L, Khan MA, He T, et al. Tripartite motif containing 28 (TRIM28) promotes breast cancer metastasis by stabilizing TWIST1 protein. *Sci Rep.* 2016; 6: 29822.
- Blume C, Jackson CL, Spalluto CM, Legebeke J, Nazlamova L, Conforti F, et al. A novel ACE2 isoform is expressed in human respiratory epithelia and is upregulated in response to interferons and RNA respiratory virus infection. *Nature genetics.* 2021; 53: 205-14.
- Zipeto D, Palmeira JDF, Arganaraz GA, Arganaraz ER. ACE2/ADAM17/TMPRSS2 Interplay May Be the Main Risk Factor for COVID-19. *Front Immunol.* 2020; 11: 576745.
- Hoffmann M, Kleine-Weber H, Schroeder S, Kruger N, Herrler T, Erichsen S, et al. SARS-CoV-2 Cell Entry Depends on ACE2 and TMPRSS2 and Is Blocked by a Clinically Proven Protease Inhibitor. *Cell.* 2020; 181: 271-80 e8.
- Bourgonje AR, Abdulla AE, Timens W, Hillebrands JL, Navis GJ, Gordijn SJ, et al. Angiotensin-converting enzyme 2 (ACE2), SARS-CoV-2 and the pathophysiology of coronavirus disease 2019 (COVID-19). *J Pathol.* 2020; 251: 228-48.
- Penn I, Starzl TE. Immunosuppression and cancer. *Transplant Proc.* 1973; 5: 943-7.
- Yang K, Sheng Y, Huang C, Jin Y, Xiong N, Jiang K, et al. Clinical characteristics, outcomes, and risk factors for mortality in patients with cancer and COVID-19 in Hubei, China: a multicentre, retrospective, cohort study. *Lancet Oncol.* 2020; 21: 904-13.
- Zarifkar P, Kamath A, Robinson C, Morgulchik N, Shah SFH, Cheng TKM, et al. Clinical Characteristics and Outcomes in Patients with COVID-19 and Cancer: a Systematic Review and Meta-analysis. *Clin Oncol (R Coll Radiol).* 2021; 33: e180-e91.
- Yang F, Shi S, Zhu J, Shi J, Dai K, Chen X. Clinical characteristics and outcomes of cancer patients with COVID-19. *J Med Virol.* 2020; 92: 2067-73.
- Zhang H, Han H, He T, Labbe KE, Hernandez AV, Chen H, et al. Clinical Characteristics and Outcomes of COVID-19-Infected Cancer Patients: A Systematic Review and Meta-Analysis. *J Natl Cancer Inst.* 2021; 113: 371-80.
- Katopodis P, Anikin V, Randeva HS, Spandidos DA, Chatha K, Kyrou I, et al. Pancancer analysis of transmembrane protease serine 2 and cathepsin L that mediate cellular SARS-CoV2 infection leading to COVID-19. *Int J Oncol.* 2020; 57: 533-9.
- Cheng J, Zhou J, Fu S, Fu J, Zhou B, Chen H, et al. Prostate adenocarcinoma and COVID-19: The possible impacts of TMPRSS2 expressions in susceptibility to SARS-CoV-2. *J Cell Mol Med.* 2021; 25: 4157-65.
- Kermani NZ, Song WJ, Badi Y, Versi A, Guo Y, Sun K, et al. Sputum ACE2, TMPRSS2 and FURIN gene expression in severe neutrophilic asthma. *Respir Res.* 2021; 22: 10.
- Padmanabhan P, Desikan R, Dixit NM. Targeting TMPRSS2 and Cathepsin B/L together may be synergistic against SARS-CoV-2 infection. *PLoS Comput Biol.* 2020; 16: e1008461.